JOURNAL OF combinatorial CHEMISTRY

Article

A Combinatorial Approach to the Study of Particle Size Effects on Supported Electrocatalysts: Oxygen Reduction on Gold

Samuel Guerin, Brian E. Hayden, Derek Pletcher, Michael E. Rendall, and Jens-Peter Suchsland

J. Comb. Chem., **2006**, 8 (5), 679-686• DOI: 10.1021/cc060041c • Publication Date (Web): 22 July 2006

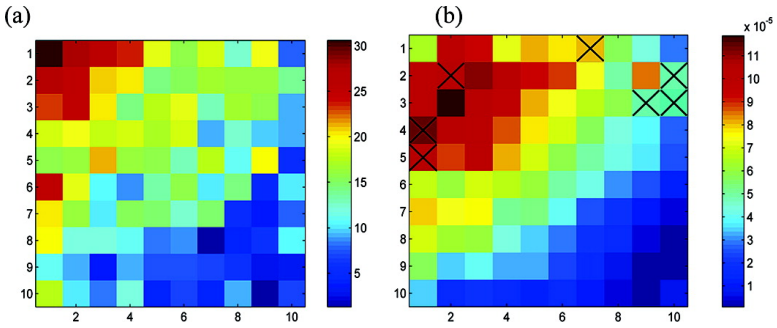

More About This Article

Additional resources and features associated with this article are available within the HTML version:

- Supporting Information
- Links to the 8 articles that cite this article, as of the time of this article download
- Access to high resolution figures
- Links to articles and content related to this article
- Copyright permission to reproduce figures and/or text from this article

View the Full Text HTML

Journal of Combinatorial Chemistry is published by the American Chemical Society.
1155 Sixteenth Street N.W., Washington, DC 20036

A Combinatorial Approach to the Study of Particle Size Effects on Supported Electrocatalysts: Oxygen Reduction on Gold

Samuel Guerin, Brian E. Hayden,* Derek Pletcher, Michael E. Rendall, and Jens-Peter Suchsland

School of Chemistry, University of Southampton, Southampton SO17 1BJ, UK

Received April 3, 2006

A novel high-throughput technique has been developed for the investigation of the influence of supported metal particle size and the support on electrocatalytic activity. Arrays with a gradation of catalyst particle sizes are fabricated in a physical vapor deposition system that also allows selection of the support material. Simultaneous electrochemical measurements at all electrodes in the array, together with determination of the actual particle size distribution on each of the electrodes by transmission electron microscopy (TEM), then allows rapid determination of the activity as a function of catalyst center size. The procedure is illustrated using data for the reduction of oxygen on gold nanoparticles supported on both substoichiometric titanium dioxide (TiO_x) and carbon and the conclusions are verified using voltammetry at rotating disk electrodes. Gold centers with diameters in the range 1.4−6.3 nm were investigated and it is demonstrated that, with both supports, the catalytic activity for oxygen reduction decays rapidly for particle sizes below 3.0 nm. This may be observed as a decrease in current at constant potential or an increase in the overpotential for oxygen reduction.

Introduction

Combinatorial screening is rapidly gaining popularity for optimizing the composition of materials for specific physical or chemical properties. Several examples[1−6] concern the selection of electrocatalyst or battery materials. Recently, a physical vapor deposition system has been developed for the high-throughput synthesis of thin film materials. It employs source shutters to achieve controlled gradients of depositing elements across a substrate or an array of pads.[7,8] This allows, for example, the synthesis of a compositional library of alloys. The system has been applied to the optimization of Pd/Pt/Au electrocatalysts when the substrate was a 10 × 10 array of individually addressable Au electrodes on a silicon nitride-covered silicon substrate.[9]

This paper describes the application of arrays of electrodes fabricated in the high-throughput physical vapor deposition (HT-PVD) system to the study of the influence of supported metal particle size and the support on electrocatalyst activity. Arrays with a gradation of metal center size on both carbon or substoichiometric titania (TiO_x) supports were fabricated and characterized.[10] To further verify the conclusions, rotating disk electrodes with the same supports and particle sizes were also prepared[10] and used for conventional voltammetry. This is the first time that high-throughput synthesis or screening techniques have been applied to the optimization of particle size in catalysis.

The system selected for study was the cathodic reduction of oxygen in aqueous acid on gold centers deposited on either carbon or substoichiometric titania (TiO_x). Despite being known as a poor catalyst for the $4e^-$ reduction, this system was chosen for a number of reasons. First, in general, the reduction of oxygen is an important reaction in fuel cells and other technologies and it has been widely studied[11,12] including Au as bulk metal,[13,14] thin layers, and particles on other substrates (although the particle diameters in all these papers are all large compared to those studied in the work reported here).[15−27] Second, the reduction of oxygen is reported to occur at a potential where the gold metal is free from both oxidized and reduced species (unlike, for example, Pt). Third, the separation in the potentials for oxygen reduction and the gold/gold oxide peaks was expected to give an in situ indication of the real surface area of the gold surfaces. Finally, small centers of Au on oxide supports such as TiO_x have recently been shown to have unique properties for catalysis; unlike bulk gold, such surfaces show very high activity for a number of gas-phase oxidations.[28−32] It was therefore considered interesting to determine whether this effect extended to small Au centers when acting as an electrocatalyst in aqueous solution. In this paper, the focus is on oxygen reduction but oxidation reactions are also being investigated. Below a certain particle diameter, it is generally recognized that electrocatalytic activity is influenced by catalytic center size and crystal face orientation; such effects have been reviewed.[33−36]

Experimental Section

Electrodes. Each array consisted of 10 × 10 gold electrodes (1 mm × 1 mm), each with individual electrical contact tracks to external contacts at the edges of the silicon nitride capped silicon wafer (31.8 mm × 31.8 mm). The gold electrodes were first coated with a uniform layer of carbon

* To whom correspondence should be addressed. Tel.: 44 (0)2380 592776. Fax: 44 (0)2380 596805. E-mail: beh@soton.ac.uk.

10.1021/cc060041c CCC: $33.50
Published on Web 07/22/2006

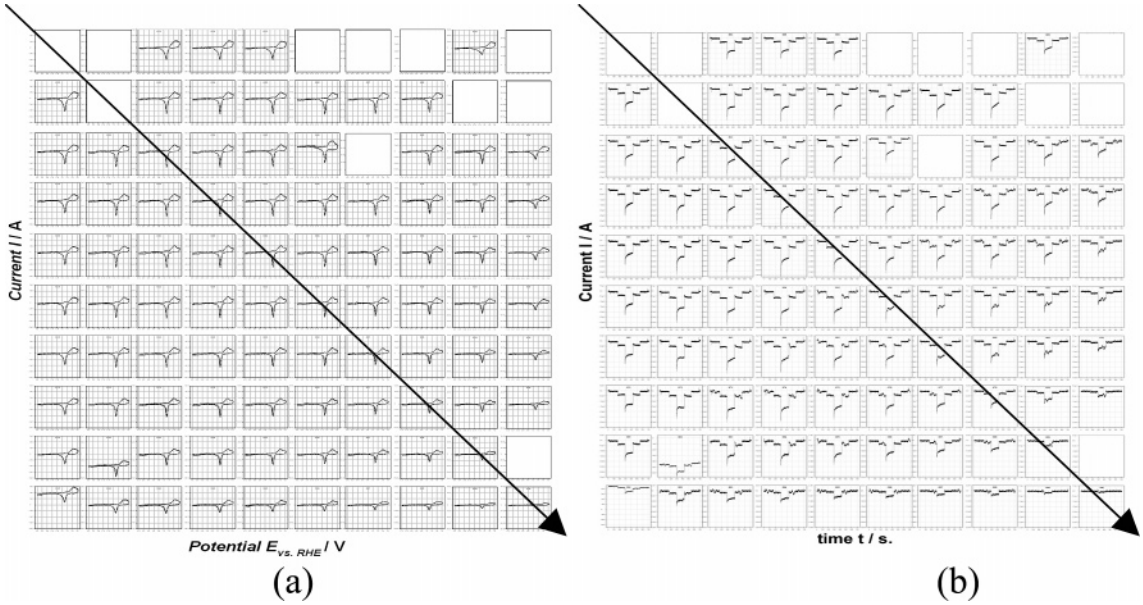

Figure 1. (a) Cyclic voltammetry (ν =100 mV s^{-1}, between 0.00 and +1.63 V) on a 100 electrode array of carbon-supported gold particles in argon-purged solution. (b) Oxygen reduction at the same array electrode as determined by potential step measurements from 0.80 V (baseline, 60 s) to 0.50 V (90 s), 0.40 V (90 s), and 0.3 V (90 s) in oxygen-saturated solution. All measurements were made in 0.5 M $HClO_4$ electrolyte at room temperature. The arrows indicate the direction of the graduated flux; in this array the upper left-hand corner corresponds to a nominal gold thickness of 1.8 nm and the lower right-hand corner to a nominal thickness of 0.21 nm.

(typical thickness 30−60 nm) or TiO_x (typical thickness 65−85 nm with an underlying thin film of titanium of ∼12 nm to ensure adhesion[10] and where $x = 1.96$). Then gold was deposited with a graduated flux of Au atoms across the diagonal of the array controlled through a fixed "wedge" shutter in the HT-PVD system. These deposition procedures and sample characterizations are described in detail in the previous paper.[10] Throughout this work, it is assumed that the gold particles grow as hemispheres. The array data at TiO_x/Au were confirmed by measurements at a rotating disk electrode (RDE). The coating of the Ti RDE disks (diameter 5 mm) with TiO_x and Au particles also followed the procedures described in the previous paper.[10]

Electrochemical Measurements. The electrochemical experiments with the arrays were carried out at room temperature in a cell where the body of the working electrode compartment is made from PTFE; the array and electrical contacts can be positioned precisely and gaskets ensure a good solution seal. The Au gauze counter electrode is in a glass compartment separated from the working electrode compartment by a glass sinter. The experimental reference electrode was a commercial (Sentec) mercury/mercuric-sulfate electrode (0.5 M H_2SO_4) whose tip was placed close to the array. All potentials presented in this report, however, are reported against the reversible hydrogen electrode in 0.5 M $HClO_4$ (RHE). The electrochemical responses of the 100 electrodes in the array are measured simultaneously using a potentiostat, 100 channel current followers, and data acquisition cards controlled/monitored by a PC together with software written in the laboratory; this instrumentation has been described earlier,[6] but the sensitivity of the current followers used here were 10 μA V^{-1}. The RDE measurements where carried out in a standard three-electrode/two-compartment, glass cell with a Luggin capillary. It also had a water jacket to maintain a temperature of 298 K, water being pumped from a thermostatically controlled water bath (Grant). The same potentiostat, data acquisition system, and software were again employed. Both cyclic voltammograms (50 and 100 mV s^{-1}) and potential step experiments were carried out at both the arrays and disks. Activity for oxygen reduction was assessed using O_2 saturated 0.5 M $HClO_4$ as the solution. With the arrays, the activity was determined using a potential step sequence. The potential was held at 0.80 V for 60 s to give a baseline in the absence of oxygen reduction and then stepped to 0.50 V (90 s), 0.40 V (90 s), and 0.30 V (90 s) and then the sequence was reversed to demonstrate reproducibility. At the RDE, steady-state voltammograms were recorded between 1.00 and −0.30 V and the currents in the mixed controlled region were corrected for any influence of mass transport using a Koutecky−Levich plot.

The combinatorial electrochemical experiments are best clarified by an example. Figure 1 illustrates a convenient presentation of electrochemical experiments at an electrode array that allow a rapid preliminary assessment of the data and identification of trends; more detailed and quantitative analysis requires different presentations. The figure shows both a set of cyclic voltammograms in deoxygenated 0.5 M perchloric acid and a set of potential step experiments in oxygen-saturated 0.5 M perchloric acid. In both Figures 1a and 1b, the arrow shows the direction of the Au coverage variation with the highest coverage in the top left-hand corner and the lowest in the bottom right-hand corner (in fact, in this array the upper left-hand corner corresponds to a nominal gold thickness of 1.8 nm and the lower right-hand corner to a nominal thickness of 0.21 nm). Perpendicular to this arrow, the Au coverage should be uniform and the surfaces should be identical. In this study of particle size effects, the single array gives 19 data points since the electrodes immediately

adjacent to those on the diagonal provide intermediate particle sizes to those on the diagonal.

From the magnitude of the gold oxide formation/reduction peaks on the cyclic voltammograms of Figure 1a, it can clearly be seen that, qualitatively, the surface area of the gold centers is decreasing down the diagonal while perpendicular to the arrows the voltammograms are similar. We would, however, caution against total reliance on the charge associated with the oxide formation/reduction peaks for estimating the surface area of small gold particles; we will later present evidence that the redox behavior of such particles on some supports is complex. Similarly, it can be seen from the potential step experiments that, at least quantitatively, the oxygen reduction currents reflect this trend in surface area.

Figure 1 also shows some limitations of the cell used for the electrochemical experiments in this project. First, the blank positions in the presentation of the array shown indicate electrodes where electrical contact has been broken during positioning of the array within the cell and then sealing the cell. Second, in the oxygen reduction experiments, see Figure 1b, the electrodes at the edges of the array often give lower currents and this results from the proximity of a wall perpendicular to these electrodes. In consequence, the cell has since been redesigned to overcome these limitations and also to allow temperature control.

To demonstrate reproducibility, all experiments have been carried out 3−4 times with arrays fabricated at different times. The trends in the catalytic activities are totally reproducible and the absolute current densities varied by <20%.

Aqueous perchloric acids solutions (0.5 M) were prepared using ultrapure water (Millipore, 18 MΩ cm) and concentrated perchloric acid (GFS Chemicals, double distilled). The gases used in the experiments were argon (BOC, 99.998%) and oxygen (BOC, 99.999%).

Results

Throughout this study, the surfaces were subjected to cyclic voltammetry in deoxygenated 0.5 M aqueous perchloric acid and to both voltammetry and potential step experiments in oxygen-saturated 0.5 M aqueous perchloric acid. With the arrays of electrodes, the results were initially presented in the form presented in Figure 1; this allowed the identification of trends. More quantitative analysis of the data requires the responses to be presented in different and expanded formats and this was achieved through software based on Matlab and able to handle the large number of data files that accumulate for experiments with 10 × 10 arrays. The data at each electrode in the array could also be presented individually in expanded form or responses from different electrodes could be presented together for purposes of comparison. In addition, the software allowed calculations with the numerical data and hence quantitative interpretation. We would, however, stress that visual observation before quantitative analysis is critical to obtaining full value from the experimental data.

Figure 2 shows expansions of steady-state cyclic voltammograms for an O_2 saturated 0.5 M $HClO_4$ recorded at

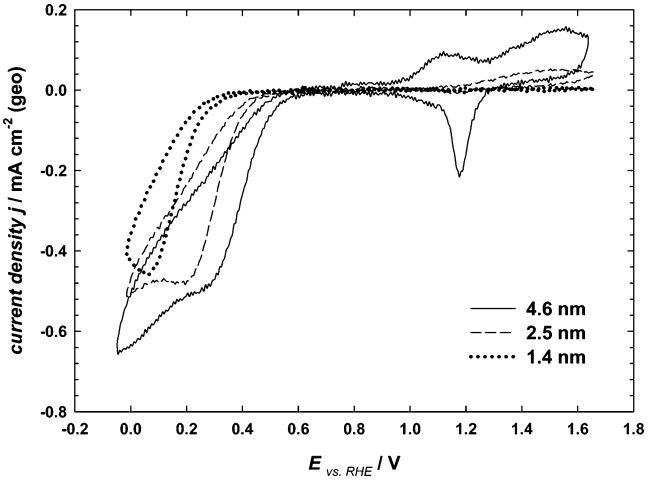

Figure 2. Cyclic voltammograms of TiO_x-supported gold particles (mean particle diameters 4.6, 2.5, and 1.4 nm) in O_2-saturated 0.5 M $HClO_4$. Potential scan rate 50 mV s^{-1}. The responses shown are the third cycle.

three electrodes in an array of Au/TiO_x electrodes. The three voltammograms correspond to surfaces with different mean particle diameters of gold. At all three surfaces, oxygen reduction is observed as an irreversible peak/wave in the potential range +0.40−0.00 V. The limiting currents are very similar (as expected for a diffusion-controlled process) but the reduction of oxygen clearly shifts to a more negative potential as the gold loading is decreased; i.e., the overpotential for O_2 reduction increases with diminishing gold loading (particle size). With the biggest particle size of gold, all features on the voltammogram are similar to those at a bulk gold electrode; the scan to more positive potentials shows a peak at +1.12 V for the oxidation of the hydrogen peroxide formed during the reduction of oxygen, and at more positive potentials, charge for the oxidation of the gold surface is observed. In addition, the peak at +1.18 V on the negative-going scan is characteristic of the reduction of the oxygen-covered surface back to gold. At the smaller particle sizes, the responses at more positive potentials are more surprising. First, the anodic current for the oxidation of hydrogen peroxide is much diminished. This is partly because less hydrogen peroxide is formed in the experiment but more importantly the oxidation appears to become more irreversible on the smaller gold particle sizes. Second, the oxidation of the gold surface appears to become more irreversible. Indeed, even with a positive limit of +1.63 V, at the smallest particles, little oxide is formed. This is most clearly evidenced by the absence of the peak for the reduction of the oxidized gold surface. These conclusions were confirmed by experiments in deoxygenated 0.5 M $HClO_4$. In this paper, however, the emphasis will be on the cathodic reduction of oxygen on gold. The oxidation and reduction of the gold surface with low loadings of gold will be discussed further in other publications. Note that the gold/gold oxide behavior on small carbon-supported gold particles is very similar to that of bulk gold for all particle sizes (Figure 1a).

The activity for oxygen reduction was assessed quantitatively using a potential step technique. The potential was stepped from +0.80 V where oxygen reduction does not occur and the gold surface is free of oxide to +0.50, +0.40,

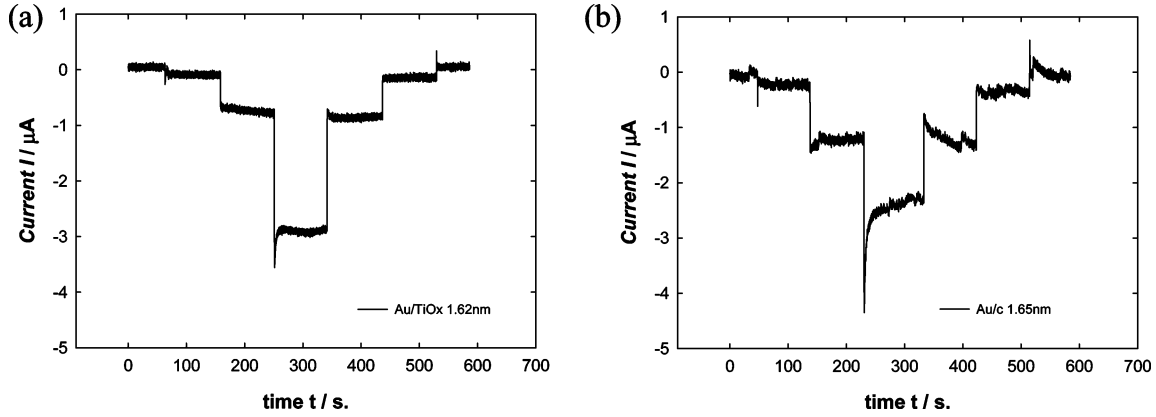

Figure 3. Enlarged presentation of the current vs time responses to a potential step sequence, 0.80 → 0.50 → 0.40 → 0.30 → 0.40 → 0.50 → 0.80 V, in O_2-saturated 0.5 M $HClO_4$ at electrodes in a 10 × 10 array with nominal gold thickness of ~1.65 nm. (a) Au on TiO_x; (b) Au on C.

and 0.30 V, each for 90 s and the direction of the step was then reversed in order to check the reproducibility of the currents. An overview of the response at one array was presented in Figure 1b but with this presentation the only immediate conclusion is that the extent of oxygen reduction increases with the amount of gold on the surface. Figure 3 illustrates expansions of the data for gold on both carbon and TiO_x taken from different arrays. In both cases, the gold coverage is equivalent to a nominal thickness of 1.65 nm. Two conclusions are clear. First, at the gold coverage shown the substrate does not appear to be a major factor in determining the rate of oxygen reduction. Second, at +0.50 and +0.40 V, the current is independent of time and therefore it may be concluded that oxygen reduction is almost fully electron-transfer-controlled. At +0.30 V, there is a small initial decay in current perhaps due to some influence of non-steady-state diffusion. The figure also confirms that when the direction of the potential steps is reversed, the same constant currents are obtained at both +0.40 and +0.50 V. The data at +0.50 V was not further analyzed because of the small magnitudes of the currents compared to the noise and the currents at +0.40 and +0.30 V were used as a measure of oxygen reduction activity below.

Oxygen reduction was also examined as a function of gold center size using rotating disk voltammetry. Figure 4 reports a set of voltammograms as a function of rotation rate for a Ti/TiO_x/Au disk (mean Au center diameter is 1.8 nm) in O_2-saturated 0.5 M perchloric acid. Each voltammogram has a well-formed wave for the reduction of oxygen with $E_{1/2}$ close to +0.20 V and a mass-transport-controlled plateau negative to 0 V. This is close to the response at a massive gold electrode, although the waves are slightly shifted toward more negative potentials. The inset shows Koutecky−Levich plots at a series of potentials and the intercepts on the *y*-axis were taken as the inverse of the kinetic current for oxygen reduction free of distortion from mass-transport control. Voltammograms were also recorded in O_2-saturated 0.5 M $HClO_4$ solution for eight further Ti rotating disk electrodes with TiO_x substrate layers but gold deposits with different particle sizes ranging from 1.4 to 4.5 nm. The voltammograms obtained at 900 rpm are reported in Figure 5. It can be seen that the limiting current density for oxygen reduction (based on the geometric area) is independent of the amount

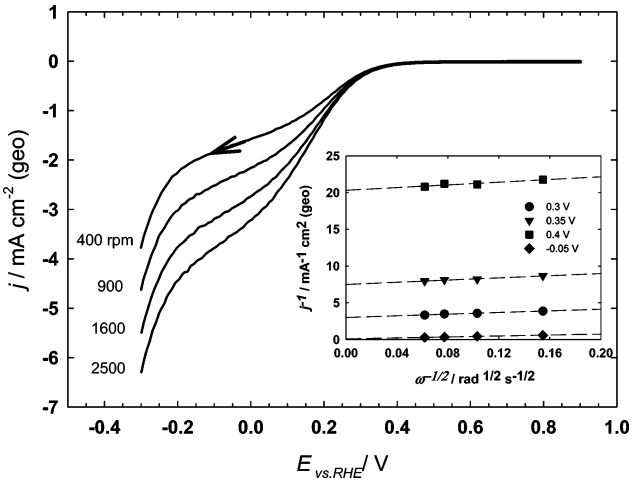

Figure 4. Steady-state polarizations for oxygen reduction on gold particles (mean particle diameter 1.8 nm) supported on a thin film (66 nm) of TiO_x (deposited on a titanium disk electrode). The insert shows the Koutecky−Levich plot for the potentials −0.05 (assumed limiting current density), 0.30, 0.35, and 0.40 V. All measurements have been made in oxygen-saturated 0.5 M $HClO_4$ at a temperature of 298 K.

of gold on the surface and hence of particle size. Also, at intermediate particle sizes of 3.1−4.5 nm, the response is very similar but with smaller particles (<2.5 nm) the reduction wave shifts to significantly more negative potentials. The kinetic currents at +0.40 and +0.30 V as determined by Koutecky−Levich plots were again taken as a measure of activity of the surfaces for oxygen reduction.

In addition, the kinetic currents as a function of potential were used to construct Tafel plots. At all surfaces studied, the log *j* vs *E* plots were linear with a slope of $(120 \pm 12\ mV)^{-1}$ and this is the Tafel slope reported for other gold surfaces in the literature.[14,15] This confirms that the mechanism for oxygen reduction at the small gold centers is the same as that at bulk gold and that the reaction is initiated by the transfer of a single electron.

The most appropriate measure of catalytic activity is the current density based on the exposed gold/electrolyte interface. To interpret the data in terms of the mean diameters of the gold centers and real surface area, it is necessary to characterize the surface structure. The characterization of the gold deposits for such an analysis was achieved by TEM

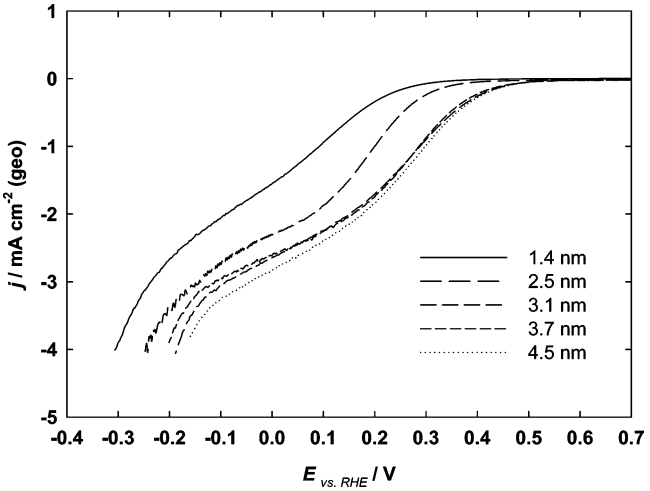

Figure 5. Steady-state polarizations ($\nu = 20$ mV s^{-1}) for oxygen reduction on Au/TiO_x RDE electrodes with different gold coverages, mean particle diameters shown on the figure. TiO_x film thickness 66 nm. Rotation rate 900 rpm. O_2-saturated 0.5 M $HClO_4$. Temperature of 298 K.

and is reported in more detail elsewhere.[10] Here, only some critical conclusions from the TEM analysis are summarized. The gold deposits with different nominal thicknesses were achieved by varying the deposition time and, of course, on both TiO_x and C substrates each deposition leads to gold centers with a distribution of sizes. Figure 6a shows the distribution of particle sizes from depositions onto a TiO_x support carried out with a flux of gold equivalent to the uniform deposition of 0.16 nm nominal thickness per minute for five deposition times between 50 and 1050 s. Clearly, the particles get larger with deposition time and the size distribution becomes broader. In contrast to the presentation in ref 10, however, data are plotted as the number density of particles with each diameter; hence, assuming that the particles are hemispherical, these data allow the calculation of the total surface area of gold exposed for each of these five surfaces. Note that the surface area was calculated from the TEM measurements of particle size and number of particles per cm^{-2}, rather than the electrochemistry and the redox behavior of the gold, because of the unusual redox behavior of titania-supported gold (see above). Figure 6b reports the results of such calculations for a large number of surfaces studied in this work; the total exposed area of gold is a smooth function of the nominal thickness. A similar curve was obtained for the Au/C deposits.

The software allows the oxygen reduction activities at the arrays of electrodes to be presented in a number of ways. Figure 7 presents the data from a 10×10 Au/TiO_x array as contour plots. Figure 7a shows the amount of gold deposited over the array as estimated by EDS; the decrease in gold from the top left to the bottom right is clearly seen while perpendicular to the arrow the relative uniformity is apparent. Figure 7b reports the activity for oxygen reduction, in fact, the current densities for oxygen reduction at +0.30 V (based on the geometric surface are of gold exposed to the electrolyte), again as a contour plot. The correlation between the two figures is clear and it can again be seen that the oxygen reduction rate drops off with the amount of gold and hence particle diameter on the TiO_x support.

In this study, however, we wished to include array and RDE results in the same presentation and to emphasize the influence of gold particle size on the oxygen reduction activity. Figure 8 therefore summarizes the data from both the array and rotating disk electrode experiments for the activity of the surfaces (TiO_x/Au) for oxygen reduction as a function of the mean particle diameter. The results are shown for two potentials, +0.4 and +0.3 V. Throughout the current density is based on the total real area of gold exposed to the solution as calculated from the number density and mean diameter of the gold particles as set out above. The error bars indicate (i) the standard deviation of the particle size distribution resulting from each deposition and (ii) the variation in the currents at the arrays as estimated from the standard deviation of the currents across the row of electrodes with average particle size. First, we would stress that the trends identified from the array and the rotating disk electrode experiments are identical. Second, at both potentials, the dramatic *conclusion is the loss of activity for oxygen reduction (as measured at the constant potentials) for gold centers smaller than 2 nm. In addition, the plot shows a maximum in activity at a mean diameter of 2.5−3.0 nm.* These trends were totally reproducible in experiments with

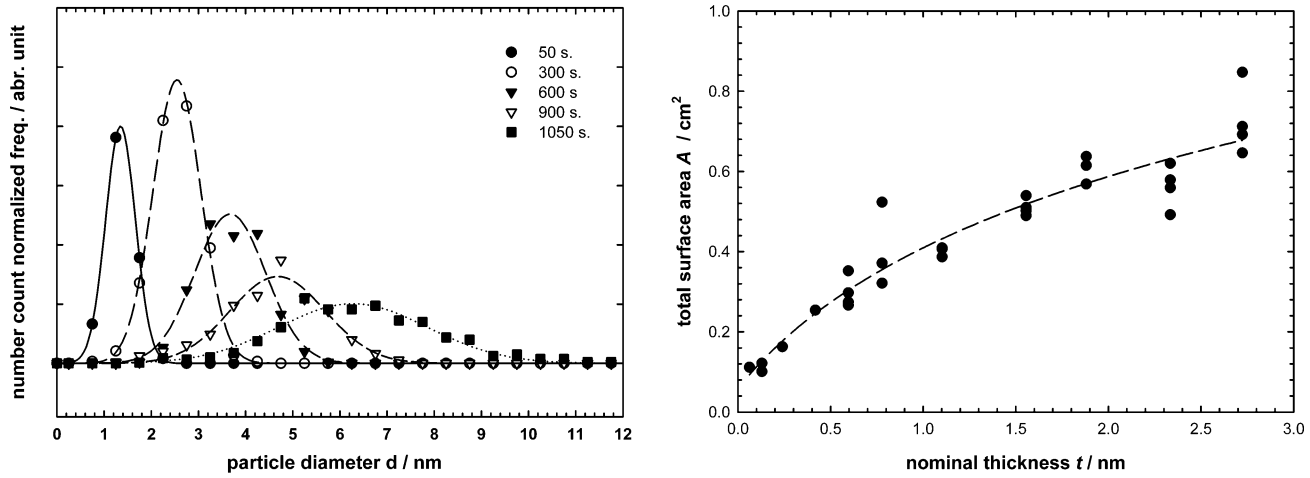

Figure 6. (a) Particle size distributions of gold particles grown on TiO_x obtained from TEM measurements. Gold deposition times are shown in the figure. The data were fitted to a normal Gaussian function. (b) The surface area of the gold calculated from the mean particle diameter and the number of particles per unit area, assuming the particles are hemispherical.

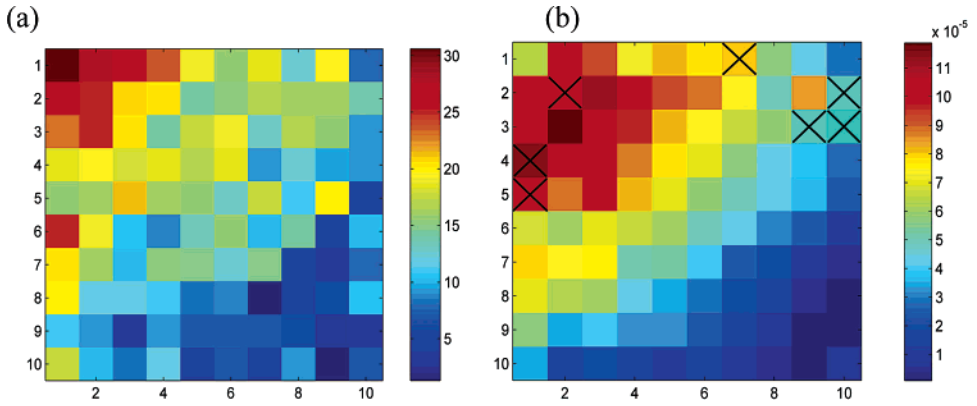

Figure 7. Comparison of (a) the amount of gold as determined by EDS during calibration (arbitrary units) and (b) the oxygen reduction current density (A cm^{-2}) (based on geometric area) at +0.3 V. 10 × 10 titania array. The nominal gold thicknesses range from 0.6 to 0.07 nm. The crosses indicate electrodes where electrical contact has been broken.

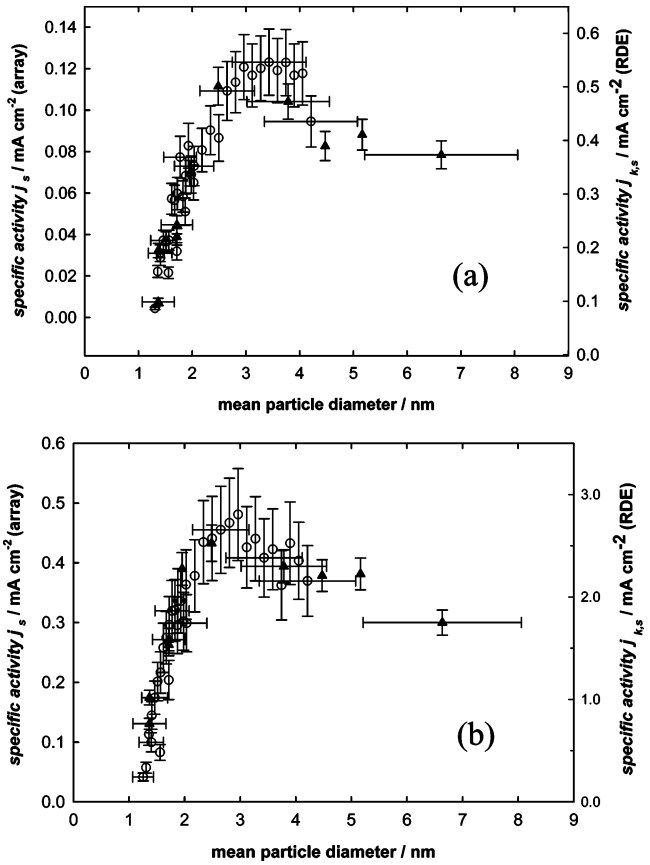

Figure 8. Specific oxygen reduction activity of TiO_x-supported gold particles at (a) 0.40 V and (b) 0.30 V vs RHE. Open circles (○) correspond to measurements on the (10 × 10) array of electrodes; full triangles (▲) correspond to the RDE measurements. The error bars along the particle size axis indicate the range of particle size (in fact, the standard deviation of the particle size) observed by TEM. The error bars on the specific activity axis reflect the standard deviation of the currents measured at the 10 electrodes on the array with a mean particle size.

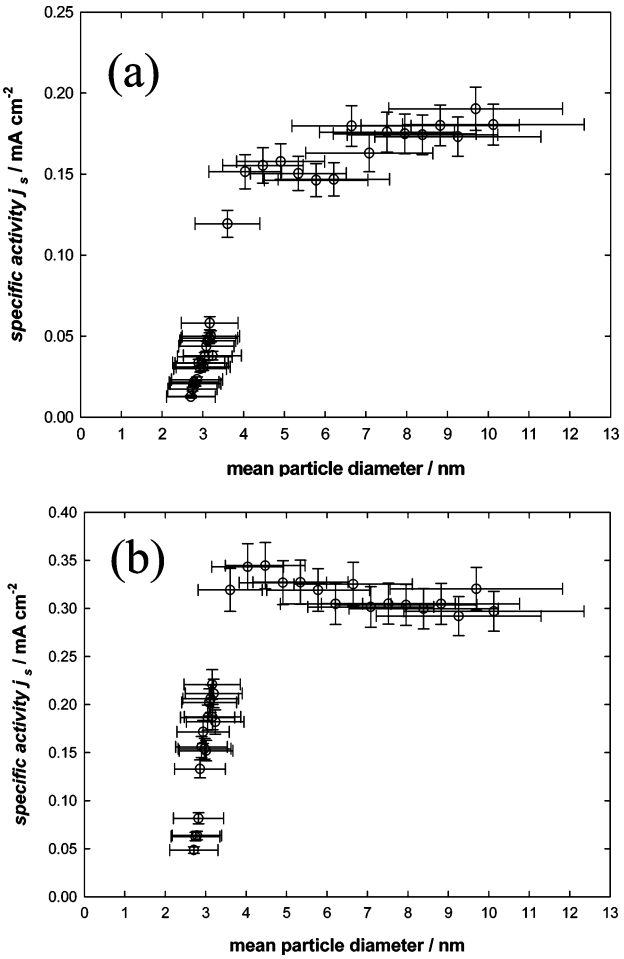

Figure 9. Specific oxygen reduction activity of carbon-supported gold particles at (a) 0.40 V and (b) 0.30 V vs RHE measured on the (10 × 10) array of electrodes. The error bars are explained in the legend to Figure 8.

four arrays fabricated at different times. The absolute difference in the magnitudes of the currents at the array and disks probably arises largely from differences in the temperatures in the experiments (i.e., room temperature, i.e., typically 288 K, for the arrays and 298 K for the RDE).

Figure 9 reports the analogous plots of activity for oxygen reduction activity versus particle size for gold on carbon resulting from array experiments. The overall picture is similar to a *sharp dropoff in activity again observed for particles with diameters below 3 nm*. No maximum is, however, observed in the particle size dependence of specific activity with a carbon substrate. It should be pointed out that the TEM analysis of the Au on C surfaces showed significant differences in nucleation and growth characteristics compared to those for Au on TiO_x.[10] In particular, it was more difficult to create surfaces with very small Au centers; the formation of centers was followed by rapid growth to a critical size

(~2.6 nm). In consequence, while the decay in activity on the smaller centers is clear, the precise particle size where the decrease in activity occurs is less certain. The TiO_x surface appears to stabilize smaller centers.

Discussion

The main purpose of this paper was to establish the combinatorial approach to the study of particle size effects in catalysis/electrocatalysis. The results clearly achieve this goal. The arrays used in this work have 100 electrodes fabricated as a single unit. They give 19 data points for different catalyst center dimensions while the other electrodes in the 10×10 array give simultaneous confirmation of the reproducibility of the recorded data. Obtaining the same volume of data from individual electrodes would require substantially more fabrication time and costs as well as many more electrochemical experiments. The rotating disk experiments were carried out to demonstrate that the trends in activity were independent of the approach used to measure the activity. Indeed, the trends in the activity vs particle size data from the array and the disk electrodes are identical.

The catalytic activity for oxygen reduction was quantified both through observation of the overpotential for oxygen reduction and by measurement of the kinetic current at two potentials. All measurements show that, above a critical center diameter, the catalytic activity becomes independent of center dimensions. On the other hand, there can be no doubt that small particles of gold with diameters below 2.5−3.0 nm are less active for oxygen reduction, independent of the supporting material. Moreover, this loss in activity at small centers was observed with both TiO_x and C at substrates.

It is interesting to note that a similar loss in specific activity in the oxygen reduction reaction in acid solution is observed for small Pt centers on a carbon support (ref 6 and references therein). With both gold and platinum catalysis, the optimum loading is determined by the balance between the need for high metal dispersion (maximizing surface area and metal utilization) and the loss of activity for small particles. This results in a maximum in the mass normalized catalyst activity at around 3 nm. If general, this is an important observation for the design and manufacture of electrocatalysts; catalyst centers need to be a critical size but above this size, there is only an economic penalty in using more precious metal.

In the case of titania-supported gold, there is evidence for a maximum in the specific activity of the gold particles at 2.5−3.0 nm. The smaller particles require a larger overpotential to drive the reduction of gold; see Figure 5. On the other hand, we have found no evidence for a change in the mechanism for oxygen reduction with particle size or support. The maximum in electrocatalytic activity is observed for Au particle sizes which are optimal for catalyzing a number of gas-phase oxidations[28−32] where titania is used as a support. This is interesting but at the present stage we can only speculate whether the changes in activity for cathodic oxygen reduction and gas-phase oxidations share a common cause. The explanations in the literature for the increase in rate of the gas-phase oxidations differ markedly. Different authors ascribe the effect to enhancement in the density of special sites especially step sites,[37] strong electronic interactions between the gold particles and oxide substrate,[38−40] distinctive electronic properties of the gold centers,[41] and spillover and chemistry at the interface of the gold and oxide.[42] In addition to this, the detailed surface mechanism for ORR is not fully understood, although it is clear that the interaction of the oxygen with the gold particle will result in differences in the steady-state oxygen coverage and the rate of oxygen dissociation, both of which will influence the rate of ORR. We do observe strong particle size dependence in the surface redox behavior of the supported gold particles, and we will report these observations in detail elsewhere.

Acknowledgment. The authors wish to acknowledge GM for their financial support of this program and F.T. Wagner and H.A. Gasteiger for helpful discussions of the results.

References and Notes

(1) Reddington, E.; Sapienza, A.; Garau, B.; Viswanathan, R.; Sarangapani, S.; Smotkin, E. S.; Mallouk, T. E. *Science* **1998**, *280*, 1735.
(2) Morris, N. D.; Mallouk, T. E. *J. Am. Chem. Soc.* **2002**, *124*, 11114.
(3) Chen, G. Y.; Delafuente, D. A.; Sarangapani, S.; Mallouk, T. E. *Catal. Today* **2001**, *67*, 341.
(4) Sun, Y. P.; Buck, H.; Mallouk, T. E. *Anal. Chem.* **2001**, *73*, 1599.
(5) Spong, A. D.; Vitens, G.; Guerin, S.; Hayden, B. E.; Russell, A. E.; Owen, J. R. *J. Power Sources* **2003**, *119*−*121*, 778.
(6) Guerin, S.; Hayden, B. E.; Lee, C. E.; Mormiche, C.; Owen, J. R.; Russell, A. E.; Theobald, B.; Thompsett, D. *J. Comb. Chem.* **2004**, *6*, 149.
(7) Guerin, S.; Hayden, B. E. *J. Comb. Chem.* **2006**, *8*, 66.
(8) Hayden, B. E.; Guerin, S. A Vapour Deposition Method. Patent Application (2004) PCT/GB2004/004255.
(9) Guerin, S.; Hayden, B. E.; Lee, C. E.; Mormiche, C.; Russell, A. E. Submitted to *J. Phys. Chem. B.*
(10) Guerin, S.; Hayden, B. E.; Pletcher, D.; Rendall, M. E.; Suchsland, J.-P.; Williams, L. Previous paper.
(11) Hoare, T. P. *The Electrochemistry of Oxygen*; Interscience: New York, 1968.
(12) Kinoshita, K. *Electrochemical Oxygen Technology*; John Wiley & Sons: New York, 1992.
(13) Adzic, R. R.; Strbac, S.; Anastasijevic, N. *Mater. Chem. Phys.* **1989**, *22*, 349.
(14) Maruyama, J.; Inaba, M.; Ogumi, Z. *Electrochim. Acta* **1999**, *45*, 415.
(15) Sarapuu, A.; Tammesvski, K.; Tenno, T. T.; Sammelselg, V.; Kontturi, K.; Schiffrin, D. J. *Electrochem. Commun.* **2001**, *3*, 446.
(16) El-Deab, M. S.; Ohsaka, T. *Electrochem. Commun.* **2002**, *4*, 288.
(17) Zhang, Y.; Asahina, S.; Yoshihara, S.; Shiraksshi, T. *Electrochim. Acta* **2003**, *48*, 741.
(18) El-Deab, M. S.; Ohsaka, T. *J. Electroanal. Chem.* **2003**, *533*, 107.
(19) El-Deab, M. S.; Okajima, T.; Ohsaka, T. *J. Electrochem. Soc.* **2003**, *149*, A851.
(20) Jaramillo, T. F.; Baeck, S.-H.; Cuanya, B. R.; McFarland, E. W. *J. Am. Chem. Soc.* **2003**, *125*, 7148.
(21) Zhang, Y.; Suryanarayanan, V.; Nakazawa, I.; Yoshihara, S.; Shirakashi, T. *Electrochim. Acta* **2004**, *49*, 5235.
(22) Yagi, I.; Ishida, T.; Uosaki, K. *Electrochem. Commun.* **2004**, *6*, 773.
(23) El-Deab, M. S.; Sotomura, T.; Ohsaka, T. *J. Electrochem. Soc.* **2005**, *151*, E213.

(24) El-Deab, M. S.; Sotomura, T.; Ohsaka, T. *Electrochem. Commun.* **2005**, *7*, 29.
(25) El-Deab, M. S.; Sotomura, T.; Ohsaka, T. *J. Electrochem. Soc*. **2005**, *152*, C1.
(26) Gao, F.; El-Deab, M. S.; Sotomura, T.; Ohsaka, T. *J. Electrochem. Soc*. **2005**, *152*, A1226.
(27) Baeck, S.-H.; Jaramillo, T. F.; Kleiman-Shwarsctein, A.; McFarland, E. W. *Meas. Sci. Technol.* **2005**, *16*, 54.
(28) Haruta, M. *Catal. Today* **1997**, *36*, 153.
(29) Haruta, M.; Date, M. *Appl. Catal. A* **2001**, *222*, 427.
(30) Schmid, G.; Corain, B. *Eur. J. Inorg. Chem*. **2003**, 3081.
(31) Cameron, D.; Holliday, R.; Thompson, D. *J. Power Sources* **2003**, *118*, 298.
(32) Date, M.; Okumura, M.; Tsubota, S.; Haruta, M. *Angew. Chem.* **2004**, *43*, 2129.
(33) *Handbook of Fuel Cells, Volume 2 − Electrocatalysis*; Vielstich, W., Lamm, A., Gasteiger, H. A., Eds.; Wiley: New York, 2003.
(34) Thompsett, D. In *Fuel Cells Technology Handbook*; Hoogers, G., Ed.; CRC Press: Boca Raton, FL, 2003; pp 6−12.
(35) Markovic, N. M.; Ross, P. N. In *Interfacial Electrochemistry − Theory, Experiment and Applications*; Wieckowski, A. J., Ed.; Marcel Dekker: New York, 1999.
(36) *Catalysis and Electrocatalysis at Nanoparticle Surfaces*; Wieckowski, A. J., Savinova, E. R., Vayenas, C. G., Eds.; Marcel Dekker: New York, 2003.
(37) Boccuzzi, F.; Chiorino, A.; Manzoli, M.; Lu, P.; Akita, T.; Ichikawa, A.; Haruta, M. *J. Catal.* **2001**, *202*, 256.
(38) Yang, Z.; Wu, R.; Goodman, D. W. *Phys. Rev. B* **2000**, *61*, 14066.
(39) Lopez, N.; Norskov, J. L. *Surf. Sci.* **2002**, *515*, 175.
(40) Lopez, N.; Norskov, J. K.; Janssens, T. V. W.; Carlsson, A.; Puig-Molina, A.; Clausen, B. S.; Grunwaldt, J.-D. *J. Catal.* **2004**, *225*, 86.
(41) Chen, M. S.; Goodman, D. W. *Science* **2004**, *306*, 252.
(42) Date, M.; Okumura, M.; Tsubota, S.; Haruta, M. *Angew. Chem.* **2004**, *43*, 2129.

CC060041C